Evaporation change and global warming: The role of net radiation and relative humidity

David J. Lorenz,[1] Eric T. DeWeaver,[1] and Daniel J. Vimont[1]

Received 26 January 2010; revised 24 June 2010; accepted 12 July 2010; published 29 October 2010.

[1] The change in evaporation over the oceans in climate models is analyzed from the perspective of air-sea turbulent fluxes of water and energy. The results challenge the view that the change in evaporation is predominantly constrained by the change in the net radiation at the surface. For fixed net radiation change, it is found that (1) robust increases in near-surface relative humidity and (2) robust decreases in turbulent exchange coefficient lead to a substantial reduction in evaporation below the rate of increase implied by the net radiation alone. This reduction of evaporation is associated with corresponding changes in the sensible heat flux. In addition, a net imbalance in the surface energy budget under transient greenhouse gas forcing provides a further reduction in the evaporation change in climate models. Further results also suggest that it might be more physical to view the evaporation change as a function of relative humidity change rather than net radiation. In this view, the relative humidity controls the net surface shortwave radiation through changes in low-level cloudiness and the temperature controls the net surface radiation through the changes in longwave radiation. In addition, the results demonstrate the dominant role of both the air-sea temperature difference and relative humidity over, for example, wind speed in reducing the evaporation change in climate models below the Clausius-Clapeyron rate.

Citation: Lorenz, D. J., E. T. DeWeaver, and D. J. Vimont (2010), Evaporation change and global warming: The role of net radiation and relative humidity, *J. Geophys. Res.*, *115*, D20118, doi:10.1029/2010JD013949.

1. Introduction

[2] In response to global warming, climate models predict that global-mean precipitation will increase with surface air temperature at a rate of about 1% to 3% per degree Kelvin [*Boer*, 1993; *Allen and Ingram*, 2002; *Allan and Soden*, 2007]. This change in precipitation is substantially smaller than the change in atmospheric water vapor, which increases at the Clausius-Clapeyron (CC) rate of 6% to 7% per Kelvin [*Boer*, 1993; *Allen and Ingram*, 2002; *Held and Soden*, 2006]. Recently, *Wentz et al.* [2007] have reported trends in "observed" precipitation that are about three times larger than the climate models and more in line with the CC rate. The difference between modeled and observed estimates of precipitation change indicate that (1) models are lacking the essential physical processes that generate the correct changes in precipitation [*Wentz et al.*, 2007; *Allan and Soden*, 2007], (2) observed estimates of global precipitation are inadequate for determining trends in precipitation due to global warming [*Previdi and Liepert*, 2008; *Lambert et al.*, 2008], or (3) precipitation variations in the observed record are not yet dominated by the precipitation response to global warming [*Allen and Ingram*, 2002; *Previdi and Liepert*, 2008].

[3] Why do models predict an increase in precipitation that is substantially below the CC rate? The answer appears be to the dominant role that the hydrologic cycle plays in the global energy budget [*Boer*, 1993; *Allen and Ingram*, 2002; *Pierrehumbert*, 2002; *Lambert and Allen*, 2009]. In the troposphere, the dominant balance in the time-mean atmospheric energy budget is between radiative cooling and latent heating from precipitation, and as such changes in precipitation are generally assumed to be constrained by the ability of the atmosphere to radiate away heat generated by condensation [*Allen and Ingram*, 2002]. This view generally assumes a negligible change in the sensible heat flux from the surface to the atmosphere and therefore assumes that large trends in "observed" precipitation must be accompanied by large changes in the net radiative cooling of the atmosphere.

[4] Our analysis differs from the analysis in *Allen and Ingram* [2002] in that we address changes in the hydrological cycle through the *surface* energy budget rather than the atmospheric energy budget. We believe that an analysis in terms of the surface energy budget makes quantitative assessment of the relative roles of latent *and* sensible heat much easier. Indeed, we find that changes in the sensible heat flux are not negligible and in some climate models can even be larger than the net radiation change at the surface. Formally, our consideration of the surface energy budget is the same as the atmospheric energy budget of *Allen and Ingram* [2002] if equilibrium is assumed and sensible heat

[1]Center for Climatic Research, Madison, Wisconsin, USA.

0148-0227/10/2010JD013949

Table 1. The IPCC Models Used in This Study[a]

Model (CMIP3 I.D.)	Variables	Model number in Figures 1 and 2
bccr_bcm2_0	T_a, T_s, E, S, F, r	1
cccma_cgcm3_1	T_a, T_s, E, S, F, r, u_s, v_s	2
cccma_cgcm3_1_t63	T_a, T_s, E, S, F, r, u_s, v_s	3
cnrm_cm3	T_a, T_s, E, S, F, r, u_s, v_s	4
csiro_mk3_0	T_a, T_s, E, S, r, u_s, v_s	5
csiro_mk3_5	T_a, T_s, E, S, F, r, u_s, v_s	6
gfdl_cm2_0	T_a, T_s, E, S, F, r, u_s, v_s	7
gfdl_cm2_1	T_a, T_s, E, S, F, r	8
giss_model_e_h	T_a, T_s, E, S, F, r	9
giss_model_e_r	T_a, T_s, E, S, r, u_s, v_s	10
iap_fgoals1_0_g	T_a, T_s, E, S, F, r, u_s, v_s	11
ingv_echam4	T_a, T_s, E, S, r, u_s, v_s	12
Inmcm3_0	T_a, T_s, E, S, F, r, u_s, v_s	13
ipsl_cm4	T_a, T_s, E, S, F, r, u_s, v_s	14
miroc3_2_hires	T_a, T_s, E, S, F, r, u_s, v_s	15
miroc3_2_medres	T_a, T_s, E, S, F, r, u_s, v_s	16
mpi_echam5	T_a, T_s, E, S, F, r	17
mri_cgcm2_3_2a	T_a, T_s, E, S, F, r, u_s, v_s	18
ncar_ccsm3_0	T_a, T_s, E, S, F, r	19
ncar_pcm1	T_a, T_s, E, S, r	20
ukmo_hadcm3	T_a, T_s, E, S, F, r	21
ukmo_hadgem1	T_a, T_s, E, S, F, r	22

[a]The second column lists the variables available for that model (see text for abbreviations of the variables).

flux is ignored; the equivalence of the two methods is a direct result of zero change in the top of the atmosphere radiative heat flux.

[5] In this paper, we analyze the changes in evaporation and sensible heat in climate models from the perspective of air-sea turbulent fluxes of water and energy over the oceans:

$$E = k(q_s(T_s) - rq_s(T_a)), \tag{1}$$

$$S = kc_p(T_s - T_a), \tag{2}$$

where E is the evaporation, S is the sensible heat flux, $q_s(T)$ is the saturation specific humidity as a function of temperature, r is the relative humidity, k is the turbulent exchange coefficient that depends on wind speed and static stability, c_p is the specific heat of air at constant pressure, and the subscripts s and a refer to the sea surface temperature (SST) and near surface air temperature, respectively. Our study begins with an analysis similar to *Richter and Xie* [2008], who showed that changes in the air-sea temperature difference, relative humidity and k are important for reducing the evaporation change below the CC rate. The remainder of the paper analyzes the evaporation change by considering the constraints imposed by the surface energy budget. By recasting the energy budget in terms of the air-sea temperature difference, we show that given the change in net radiation at the surface and certain assumptions about relative humidity and k, one can calculate the equilibrium change in evaporation. Using this framework for calculating evaporation we provide answers to the following: Given the hypothesis that evaporation is primarily constrained by the net radiation at the surface [*Allen and Ingram*, 2002], are the specific mechanisms for reducing evaporation studied in *Richter and Xie* [2008] important for understanding the total change in evaporation or is the total change in evaporation primarily determined by the net radiation alone? If in fact evaporation changes at the CC rate [*Wentz et al.*, 2007], then does this mean that the net radiation at the surface must also increase at the CC rate?

[6] In this study, we first ignore constraints imposed by the energy budget and use the bulk formulae to quantify the various mechanisms that contribute to an evaporation change that is different than the CC rate (section 3). We then calculate which mechanisms are most important in climate models under global warming. In section 4, we take into account the energy budget by calculating the changes in latent and sensible heat fluxes as a function of the change in net radiation at the surface. We also quantify the relative roles of relative humidity and turbulent exchange coefficient in generating the changes in fluxes in the climate models. In section 5, we discuss the physical mechanisms that might be responsible for the relationship between radiation, relative humidity, and evaporation. In section 6, we discuss the implications of these results for climate prediction, and we discuss the possibility of detecting the changes in the air-sea temperature difference and relative humidity in the observed record.

2. Data and Methods

[7] We use output from climate change scenario integrations prepared for the IPCC Fourth Assessment Report, archived by the Program for Climate Model Diagnostics and Intercomparison at the Lawrence Livermore National Laboratory. Future climate data used here comes from the A1B scenario, a scenario in which carbon dioxide (CO_2) concentrations rise to 720 parts per million (ppm) by the year 2100 and then remain fixed for the next 200 years (i.e. until 2300). Simulations of present-day climate from the same models were obtained from the Coupled Model Intercomparison Project's "20th Century Climate in Coupled Models" (20C3M) data archive. The variables available for each model are listed in Table 1. Complete details on the forcing used in the A1B scenario is given in Appendix II of the 2001 Intergovernmental Panel on Climate Change (IPCC) report [*IPCC*, 2001]. In the results presented here, climate change is defined as the difference between the climatologies of years 2080 to 2099 in the A1B scenario and years 1980 to 1999 in the 20C3M simulations. We also look briefly at the changes observed by 2180–2199 and by 2280–2299. The analysis is restricted to the oceans between the latitudes of 60°S and 60°N because we wish to avoid the complications associated with soil moisture over land and sea ice poleward of 60°. Evaporation over oceans between 60°S and 60°N accounts for 81% of the total surface evaporation (in the climate models). Moreover, the change in evaporation over oceans between 60°S and 60°N in a given climate model is a good predictor of the change in total evaporation in that climate model (correlation = 0.87) [see also *Lu and Cai,* 2009].

[8] In the results presented here, we use the 1,000 mbar relative humidity as the surface air relative humidity. We have repeated the analysis using the 2 meter specific humidity and temperature and the results are very similar. We choose to use 1,000 mbar relative humidity instead of 2 meter specific humidity because 22 models archived relative humidity compared to 15 models that archived 2 meter specific humidity. For the saturation vapor pressure, e_s, and

the Clausius-Clapeyron rate, $\frac{1}{e_s}\frac{de_s}{dT}$, we use the function given by *Bolton* [1980]. The saturation specific humidity's in (1) are calculated assuming the surface pressure is 1,000 mbar. Because the analysis is restricted to the ocean regions, this is a good approximation.

[9] In this paper, we diagnose the temporal and spatial mean of evaporation and sensible heat using the bulk formulas (1) and (2). We sometimes average over models, too. Because (1) and (2) are nonlinear, diagnosing E and S using average k, q, and r can potentially be problematic. Therefore, for evaporation, we write

$$\overline{E} = \overline{kq_s(T_s)} - \overline{krq_s(T_a)}, \tag{3}$$

where the overbar is an average over space, model, and time and all variables depend on space, model and time. We define k using

$$k = E/(q_s(T_s) - rq_s(T_a)). \tag{4}$$

The first term on the right-hand side of (3), can be written

$$\overline{kq_s(T_s)} = k\overline{q_s(T_s)} + \overline{k'q_s'(T_s)}, \tag{5}$$

where primes denote deviations from the space, model, and time average. For monthly data the second term in (5) is −8.1% times the first. For a 12 month climatology as the time variable, the second term is −8.0% times the first, and the magnitudes of the two terms are also very similar. Therefore, all variables analyzed are 12 month climatologies. *Richter and Xie* [2008] investigated the effect of using (3) with daily data instead of a climatology and likewise found that the deviations are small. Instead of (5), $\overline{kq_s(T_s)}$ can also be written as

$$\overline{kq_s(T_s)} = \overline{k}\left(\frac{\overline{kq_s(T_s)}}{\overline{k}}\right) = k\overline{\overline{q_s(T_s)}}, \tag{6}$$

where the double overbar denotes an average of q weighted by k. The second term on the right of (3) can be written

$$\begin{aligned}\overline{krq_s(T_a)} = \overline{k}\overline{rq_s(T_a)} + k'r'\overline{q_s(T_a)} \\ + r\overline{k'q_s'(T_a)} + k\overline{r'q_s'(T_a)} + \overline{k'r'q_s'(T_a)}.\end{aligned} \tag{7}$$

The magnitudes of terms 2 through 5 on the right-hand side relative to the first are 0.87%, −7.9%, −0.63% and −0.02% for climatological data, respectively. (As before, monthly data are very similar.) Therefore we are justified in keeping the first and third terms and disregarding the rest and thus the second term on the right of (3) can also be written in the form

$$\overline{krq_s(T_a)} = \overline{k}\overline{\overline{rq_s(T_s)}}, \tag{8}$$

where, once again, the double overbar denotes an average weighted by k. For the sensible heat, the covariance terms are −0.5% times the magnitude of the mean term, and therefore we neglect these terms, and temperature averages are simple averages that are not weighted by k. Hence all terms in (1) and (2) and all terms in all equations derived from them below are understood to be simple averages except for q, which are averages weighted by the spatial, model, and temporal variability in k. When we make these approximations, the mean latent heat flux given by the bulk formula is 109.6 W m^{-2} instead of the true value of 108.7 W m^{-2} (0.78% error). To more easily compare changes in q, we weight the future q the same as the present q (i.e., we weight the future q by the 20th-century k). The error introduced by this is small: the approximate future latent heat is 114.9 W m^{-2} instead of 113.5 W m^{-2} (1.2% error).

[10] One additional detail: the calculation of k using (4) gives very large values when $(q_s(Ts) - rq_s(T_a))$ is small. Because we are using pressure level relative humidity instead of surface relative humidity, the accuracy in r is likely at least 1%. Therefore, whenever $|q_s(T_s) - rq_s(T_a)| < 0.01 \cdot q_s(T_a)$, we set the humidity difference to be $0.01 \cdot q_s(T_a)$ instead of $(q_s(T_s) - rq_s(T_a))$. This adjustment is performed 0.5% of the time.

3. Mechanisms of Evaporation Change

[11] In this section, we find the contributions of the air-sea temperature difference, the relative humidity, and k to the fractional change in evaporation over the oceans using the bulk formula for evaporation (1), and quantify those contributions in the CMIP3 climate models. Changes in any one of these three factors will cause E to deviate from the CC rate. Here, we consider these changes independent of constraints imposed by the energy budget.

[12] Precipitation and evaporation changes are typically given by the fractional change per degree temperature change: $\frac{1}{E}\frac{dE}{dT_a} = \frac{d\ln E}{dT_a}$, where E is the evaporation and T_a is the surface air temperature. By taking the derivative with respect to air temperature of (1), we decompose the total evaporation change into several components (Appendix A):

$$\frac{d\ln E}{dT_a} = \alpha - \frac{(1-\gamma)\alpha q_s(T_s)}{q_s(T_s) - rq_s(T_a)} - \frac{\frac{dr}{dT_a}q_s(T_a)}{q_s(T_s) - rq_s(T_a)} + \frac{d\ln k}{dT_a}, \tag{9}$$

where α is the CC rate ($= \frac{1}{q_s}\frac{dq_s}{dT}$) and γ is the ratio of the sea surface temperature change to the near surface air temperature change ($= \frac{dT_s}{dT_a}$). The second term on the right describes the effect of changes in the air-sea temperature difference on E, the third term on the right describes the effect of changes in the relative humidity on E, and the fourth term on the right describes the effect of the exchange coefficient (influenced by wind speed or vertical stability) on E. Note that these three terms act to increase or reduce the evaporation rate from the CC rate, α: if k and r are constant and T_s and T_a increase by the same amount (i.e., $\gamma \equiv \frac{dT_s}{dT_a} = 1$), then the evaporation increases with temperature at the CC rate.

[13] Because of the important role of the hydrologic cycle on both the surface at atmospheric energy budget, however, the E change is in general not equal to the CC rate. The constraints imposed by the energy budget are most easily seen by considering the evolution to equilibrium in response to global warming. For example, consider the case where T_s and T_a increase by the same amount. If the remaining terms in the energy budget increase at a rate less than α, then the energy budget is imbalanced and E will cool the surface (and will eventually heat the atmosphere when the water condenses). This will act to increase T_a relative to T_s so that γ will be less than one (i.e., the air-sea temperature differ-

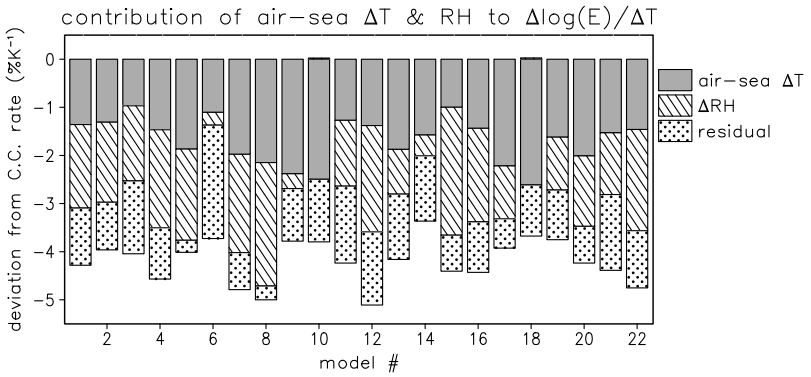

Figure 1. The contribution of the air-sea temperature difference, the relative humidity, and the residual to the fractional change in evaporation with surface air temperature for 22 climate models. The size of the bar denotes the contribution of an individual process, while the combined size of the bars gives the total reduction in evaporation change below the CC rate.

ence decreases). The reduced air-sea temperature difference will decrease E through the second term on the right side of (9) and will eventually bring the energy budget into balance. In fact, E is quite sensitive to changes in γ: substituting in the average values for $q_s(T_s)$, $q_s(T_a)$, and r over the oceans between 60°S and 60°N, we find that the second term on the right in (9) is $4.3 \cdot (1-\gamma) \cdot \alpha$. Hence a γ of 0.88 will give an E increase of 0.5α and a γ of 0.77 will give zero E increase. For the climate models, T_s increases less than T_a with a typical value for γ of 0.94.

[14] The contribution of the second, third, and fourth terms on the right-hand side of (9) to $\frac{d\ln E}{dT_a}$ are shown in Figure 1 for 22 climate models. These three terms are responsible for altering the E increase away from the CC rate, α. The size of each bar denotes the contribution of each term to $\frac{d\ln E}{dT_a}$, and the combined size of the bars give the net change in $\frac{d\ln E}{dT_a}$ from the CC rate (= 6.2 % K^{-1}). Note that for all the climate models, the net effect of these three terms is to decrease the E change below the CC rate. The results are for the oceans between the latitudes of 60°S and 60°N. For this plot, $\frac{d\ln k}{dT_a}$ is defined as the residual from the remaining terms in (9), and hence it is more uncertain.

[15] The change in the air-sea temperature difference accounts for a 1.7% K^{-1} decrease in $\frac{d\ln E}{dT_a}$ below the CC rate for the ensemble-mean. A decrease in $\frac{d\ln E}{dT_a}$ means that the air temperature is warming more than the SST. The air-sea temperature effect is negative for all climate models. The change in the relative humidity accounts for a 1.4% K^{-1} decrease in $\frac{d\ln E}{dT_a}$ below the CC rate for the ensemble-mean. A decrease in $\frac{d\ln E}{dT_a}$ means that the relative humidity is increasing. There is considerable model-to-model variability in the magnitude of the relative humidity term although 20 out of 22 models show increases in relative humidity. In addition, there appears to be a positive correlation between the relative humidity term and the total decrease in $\frac{d\ln E}{dT_a}$ below the CC rate. We will return to this point later. The residual (i.e., the estimate of $\frac{d\ln k}{dT_a}$) accounts for a 1.1% K^{-1} decrease in $\frac{d\ln E}{dT_a}$ below the CC rate for the ensemble-mean. The residual provides an estimate for changes in the turbulent exchange coefficient, which depends on the wind speed and the drag coefficient: $k = \rho C|\vec{u}|$, where ρ is the air density and C depends on static stability and surface roughness [*Stull*, 1989]. Hence the change in residual can be written as $\frac{d\ln k}{dT_a} = \frac{d\ln(\rho C)}{dT_a} + \frac{d\ln|\vec{u}|}{dT_a}$. The fact that the residual term is negative for all models might imply that there is a robust reduction in wind speed for all models in the ensemble. Looking at the actual changes in wind speed (Figure 2), however, we see that 3 out of 14 models show an increase in wind speed, yet all models have a negative residual. Moreover the changes in wind speed are rather small, with the largest decrease less than 1.0 % K^{-1}. (The wind speed is calculated by $\sqrt{u_s^2 + v_s^2}$, where u_s and v_s are daily-mean fields. There could potentially be differences between this quantity and the actual wind speed if there is substantial variability at frequencies less than a day.)

[16] The results in this section are consistent with the conclusions of *Richter and Xie* [2008], who find that changes in relative humidity and the air-sea temperature difference are the most important factors responsible for the reduction in evaporation change below the CC rate. A related study by *Lu and Cai* [2009], however, argued that changes in k are more important. We have repeated the calculations of *Lu and Cai* [2009] and our results are at odds with their conclusion that k is dominant.

4. Constraints on Evaporation Change from Energy Budget

[17] According to the view that the change in E is almost exclusively constrained by the change in net radiation at the surface, the decomposition of the E change into various components described above would not appear to be of much importance. In this view, whether the relative humidity or air-sea temperature difference is contributing to the evaporation change is irrelevant for finding the total evaporation, since the total evaporation change is simply the net radiation change (divided by the latent heat of vaporization). However, even though the sensible heat flux is a minor component to the *mean* energy budget, the *changes* in sensible heat in response to global warming are significant [*Stephens and Ellis*, 2008; *O'Gorman and Schneider*, 2008]

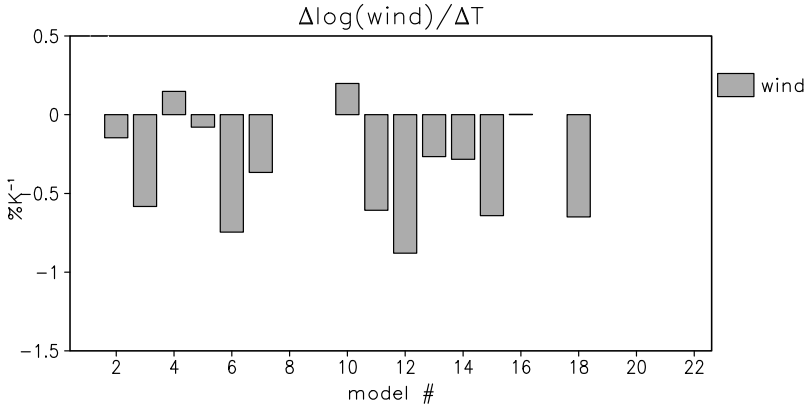

Figure 2. The change in the logarithm of the wind speed per change in surface air temperature for 14 climate models. The wind speed is averaged over the oceans from 60°S to 60°N before the logarithm.

and can in fact be larger than the changes in net radiation [*Boer*, 1993]. Indeed, we find that changes in relative humidity and k have a large effect on the partitioning of the net radiation change into the latent and sensible heat change.

[18] Here we consider the constraints on evaporation imposed by the surface energy budget:

$$c_o \frac{dT_s}{dt} = F - LE - S, \tag{10}$$

where c_o is the effective ocean heat capacity, F is the net radiation at the surface, and L is the latent heat of vaporization. The sign convention is that F is positive down and the latent and sensible heat fluxes are positive up. Under this sign convention all quantities are positive in the control climate. Given the change in any three of the above terms, the energy budget constrains the remaining term. This constraint is obvious and not very interesting.

[19] Alternatively, we can recast the energy budget so that given the change in $c_o\frac{dT_s}{dt}$, F, relative humidity (r), and k, we can calculate both LE and S. Note that a straightforward application of the energy budget constraint only determines the sum $LE + S$ and not the individual values of LE and S. The recasting of the energy budget in terms of relative humidity is useful because to first order the changes in relative humidity are zero under global warming. Therefore a reasonable first-order approximation is that relative humidity and k are constant and the energy budget is balanced (see section 4.1). If the latent heat flux is primarily constrained by the net radiation as has been suggested in the literature, then the relatively small deviations from these assumptions should not matter. When we calculate the relationship between ΔF and $L\Delta E$ using these assumptions, however, we find that relative humidity, k, and the imbalance in the energy budget *do* matter. We gradually relax all assumptions in the remaining subsections.

4.1. Fixed Relative Humidity and k

[20] Given the change of net radiation with temperature, we can calculate changes in sensible and latent heat under the assumption that relative humidity and k are constant and that the surface energy budget is balanced. In this case, the only process that can adjust to close the surface energy budget is the air-sea temperature difference. First, we start with the balanced surface energy budget:

$$F = kc_p(T_s - T_a) + kL(q_s(T_s) - rq_s(T_a)), \tag{11}$$

where F is the net shortwave and longwave radiation at the surface, c_p is the specific heat of air at constant pressure, and L is the latent heat of vaporization. Taking the derivative of (11) with respect to T_a, we have

$$\frac{dF}{dT_a} = kc_p(\gamma - 1) + kL\alpha(q_s(T_s)\gamma - rq_s(T_a)), \tag{12}$$

where $\gamma \equiv \frac{dT_s}{dT_a}$ as before. The value of γ is determined assuming that the energy budget is balanced. Solving for γ, we have

$$\gamma = \frac{\frac{dF}{dT_a} + kc_p + kL\alpha rq_s(T_a)}{kc_p + kL\alpha q_s(T_s)}. \tag{13}$$

Substituting γ in the sensible heat change ($= kc_p(\gamma - 1)$), we get the sensible heat (S) as a function of $\frac{dF}{dT_a}$:

$$\frac{dS}{dT_a} = \frac{c_p}{c_p + L\alpha q_s(T_s)}\left[\frac{dF}{dT_a} - kL\alpha(q_s(T_s) - rq_s(T_a))\right]. \tag{14}$$

The change in latent heat flux ($= \frac{dF}{dT_a} - \frac{dS}{dT_a}$) is

$$L\frac{dE}{dT_a} = \frac{L\alpha q_s(T_s)}{c_p + L\alpha q_s(T_s)}\frac{dF}{dT_a} + \frac{c_p}{c_p + L\alpha q_s(T_s)} \cdot [kL\alpha(q_s(T_s) - rq_s(T_a))]. \tag{15}$$

[21] Equations (14) and (15) give the change in sensible and latent heat assuming relative humidity and k are constant and that there is no net ocean heat uptake. All quantities in (14) and (15) except $\frac{dF}{dT_a}$ can be calculated from known quantities in the control climate of the climate models. In Figure 3a, we plot $L\frac{dE}{dT_a}$ as a function of $\frac{dF}{dT_a}$ given by (15) as well as the climate model scatter of $L\frac{dE}{dT_a}$ versus $\frac{dF}{dT_a}$. In Figure 3b, we plot the same for (14) and the climate

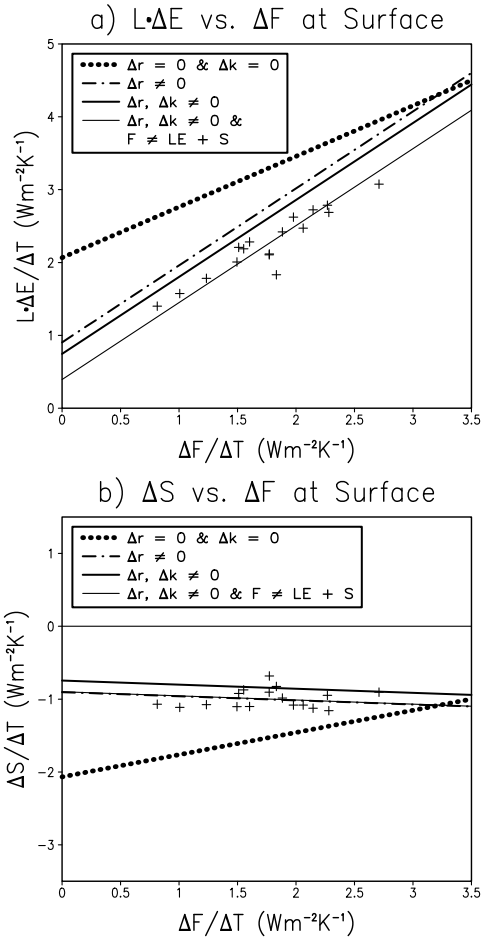

Figure 3. (a) Scatter plot of the change in latent heat flux per change in surface air temperature versus the change in net surface radiation per change in surface air temperature for 18 climate models (+ signs). The dotted line is the calculated relationship assuming relative humidity and k are constant and that the surface energy budget is balanced (15). The dashed line is the calculated relationship assuming the same as above except that relative humidity varies with temperature and radiation (18). The thick solid line adds the effect of variable k and the thin solid lines adds the effect of a residual in the surface energy budget (C4). (b) The same as Figure 3a except for sensible heat instead of latent heat.

model scatter of $\frac{dS}{dT_a}$ versus $\frac{dF}{dT_a}$. The change in E and S assuming constant relative humidity (dotted line) is drastically different from the modeled change in E and S (+ signs in Figure 3). For a 1 W m^{-2} K^{-1} change in net radiation, the change in latent heat flux for the climate models is about 1.5 W m^{-2} K^{-1} below the value for fixed relative humidity. Likewise the model reduction in sensible heat flux is substantially smaller than the reduction for fixed relative humidity. In addition, for constant relative humidity, the latent heat flux increases with temperature by over 2 W m^{-2} K^{-1} even when there is zero change in the net radiation! In this case, the change in evaporation is achieved by a small enough γ that the change in S is equal and opposite the change in E (i.e., ΔT_s is small enough compared to ΔT_a). To achieve an equivalent change in evaporation, the climate models require a 1.6 Wm^{-2} K^{-1} increase in the net radiation at the surface.

[22] To illustrate the role of the air-sea temperature difference in modulating the latent and sensible heat flux, consider the special case in which $\frac{dF}{dT_a} = 0$. Suppose an increase in greenhouse gas concentration results in an increase in downwelling longwave radiation, which warms the surface. If the warming is sufficient, the temperature-driven increase in upwelling longwave radiation will balance the downwelling radiation increase so that the net longwave radiation remains unchanged despite the warming, hence $\frac{dF}{dT_a} = 0$. For a unique value of γ, the warmer surface temperature results in an increase in evaporative heat flux, which is exactly balanced by a decrease in sensible heat flux, so that the surface energy budget remains in balance. The existence of a solution to (15) with $\frac{dF}{dT_a} = 0$ is possible because of the different dependencies of E and S on the air-sea temperature difference; the value of γ that satisfies (15) with $\frac{dF}{dT_a} = 0$ can be obtained from (13). Since $r < 1$ and $T_a < T_s$ in the climatology, (13) implies that $\gamma < 1$ for $\frac{dF}{dT_a} = 0$. The more general conditions for which $\gamma < 1$ can be found by setting the expression on the right-hand side in (13) less than one and simplifying. This leads to the condition that $\gamma < 1$ whenever $\frac{dF}{dT_a} < \alpha LE$ = CC rate. Hence, under the assumptions of this section, one expects $\Delta T_s < \Delta T_a$ whenever the net radiation change is less then the CC rate. The exact condition for $\Delta T_s < \Delta T_a$ is modified when we relax the assumptions of this section, but the basic result that $\Delta T_s < \Delta T_a$ whenever the change in net radiation is sufficiently small compared to the CC rate still holds.

[23] In the discussion above, we assume relative humidity and k are fixed, but we allow the air-sea temperature difference to vary in order to bring the latent and sensible heat change into equilibrium with the net radiation change. We do not consider the alternative scenario where the air-sea temperature difference is fixed while either the relative humidity or k are allowed to vary to bring the energy budget into balance. The reason we let γ adjust to bring the energy budget into balance is that imbalances in the energy budget lead directly to changes in the air-sea temperature difference. For example, if the sum of the latent and sensible heat change is greater than the radiation change, then the excess latent and sensible heat fluxes will heat the atmosphere and cool the surface, which is equivalent to a decrease in γ. This decrease in γ will decrease both the latent and sensible heat fluxes and therefore bring the energy budget into balance. In contrast to the obvious impact of latent and sensible heat fluxes on γ, the impact of latent and sensible heat changes on either relative humidity or k is much less certain and indirect. Hence we regard the relative humidity and k as externally imposed parameters and we allow γ to adjust to these imposed parameters in order to bring the energy budget into balance.

[24] In the discussion above, we also take the change in net radiation at the surface as given and allow the air-sea temperature difference to adjust so that the latent and sensible heat fluxes close the energy budget. In Appendix B, we discuss the validity of the assumption that the net surface radiation is unaffected by changes in the air-sea temperature difference.

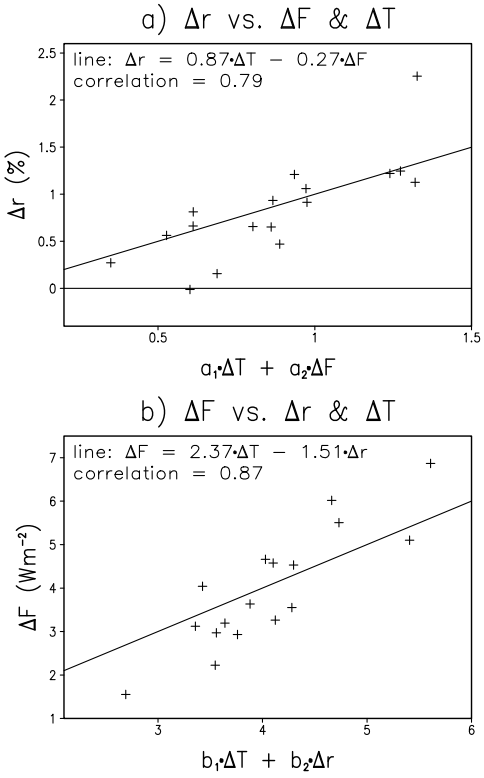

Figure 4. (a) The change in relative humidity versus $a_1\Delta T_a + a_2\Delta F$, where a_1 and a_2 are calculated from a least squares fit with no intercept. (b) The change in net radiation at the surface versus $b_1\Delta T_a + b_2\Delta r$, where b_1 and b_2 are calculated from a least square fit with no intercept. For both panels, + signs are for model results, and the solid line is the linear least squares fit.

4.2. Variable Relative Humidity and k

[25] Clearly the changes in relative humidity and k observed in the climate models are having a profound effect on the evaporation change due to global warming. To calculate the effect of relative humidity on the latent and sensible heat, we must find how relative humidity varies with temperature. We calculate the relationship between relative humidity change and temperature change using linear regression. It turns out that a significantly larger portion of the modeled variability in Δr can be "explained" by linear regression when we include ΔF as well as ΔT as predictors: $\Delta r = a_1\Delta T_a + a_2\Delta F$. (Note that the linear fit has no intercept. Thus, both the intermodel variability and the ensemble-mean change affect the value of a_1 and a_2.) The linear fit has a correlation of 0.79 with $a_1 = 0.87\%\ \mathrm{K}^{-1}$ and $a_2 = -0.27\%\ \mathrm{W}^{-1}\ \mathrm{m}^2$ (Figure 4). The coefficients in front of ΔT_a and ΔF define the values for $\frac{\partial r}{\partial T_a}$ and $\frac{\partial r}{\partial F}$, respectively. We then proceed to take the derivative of (11) with respect to T_a, replacing $\frac{dr}{dT_a}$ with $\frac{\partial r}{\partial F}\frac{dF}{dT_a} + \frac{\partial r}{\partial T_a}$.

[26] After some algebra, γ and the sensible and latent heat changes with variable relative humidity are

$$\gamma = \hat{\gamma} + \frac{Lq_s(T_a)\left(\frac{\partial r}{\partial T_a} + \frac{\partial r}{\partial F}\frac{dF}{dT_a}\right)}{c_p + L\alpha q_s(T_s)}, \tag{16}$$

$$\frac{dS}{dT_a} = \frac{d\hat{S}}{dT_a} + \frac{c_p k L q_s(T_a)}{c_p + L\alpha q_s(T_s)}\left[\frac{\partial r}{\partial T_a} + \frac{\partial r}{\partial F}\frac{dF}{dT_a}\right], \tag{17}$$

$$L\frac{dE}{dT_a} = L\frac{d\hat{E}}{dT_a} - \frac{c_p k L q_s(T_a)}{c_p + L\alpha q_s(T_s)}\left[\frac{\partial r}{\partial T_a} + \frac{\partial r}{\partial F}\frac{dF}{dT_a}\right], \tag{18}$$

where the hat refers to the corresponding quantities in (13), (14), and (15), which assume that the relative humidity is constant.

[27] Equations (17) and (18) give the change in sensible and latent heat with variable relative humidity. Including the effect of relative humidity change (Figure 3, dashed line) brings the calculated latent and sensible heat fluxes into closer agreement with the climate models. The intercept of the line is reduced because $\frac{dr}{dT_a} > 0$. The slope of the line, which has been increased by a negative $\frac{\partial r}{\partial F}$, is now basically the same as the climate models (this is the indirect effect; the negative $\frac{\partial r}{\partial F}$ reduces the relative humidity increase for a given positive change in F). For the values of $\frac{dF}{dT_a}$ in the climate models, $\frac{\partial r}{\partial T_a} + \frac{\partial r}{\partial F}\frac{dF}{dT_a} > 0$, which means r increases—leading to a reduction in E compared to the case of fixed r. Looking at (17) and (18), we see that S increases by the same amount that LE decreases when r is allowed to vary.

[28] Even after taking into account changes in r, however, there is still a net positive latent heat flux bias of about 0.5 W m^2 K^{-1} relative to the climate models. There are two reasons for the deviation of the variable relative humidity line from the climate models: (1) the turbulent exchange coefficient, k, changes, and (2) the energy budget (11) is not exact because climate model integrations are non-equilibrium greenhouse gas simulations and the oceans equatorward of 60°S and 60°N are not a closed system. In fact, the imbalance in the energy budget is large enough that an inspection of Figure 3 shows that $L\Delta E + S$ does not equal ΔF for the climate models.

[29] When we take into account the fact that k changes and that the energy budget is not balanced (Appendix C), the systematic biases in Figure 3 disappear. For the latent heat, k changes the intercept by −0.15, and the energy budget imbalance changes the intercept by −0.36. For the sensible heat, these two effects cancel: k changes the intercept by 0.15 and the energy budget imbalance changes the intercept by −0.15. The slopes and intercepts of the lines under the various assumptions described above are given in Table 2. Note that after taking account all effects on the latent heat change, the slope and intercept are close to one and zero, respectively (i.e.. $L\frac{dE}{dT_a} \approx \frac{dF}{dT_a}$). As we have seen above, however, this is a consequence of the net imbalance in the surface energy budget, the particular changes in relative humidity and k in the climate models, and the subsequent adjustment of the air-sea temperature difference that brings the energy budget back into balance.

4.3. Effect of Decreasing Relative Humidity

[30] To demonstrate the potential importance of the near surface relative humidity changes, consider the hypothetical case where the relative humidity *decreases* with temperature by an amount equal and opposite to the simulated increase (i.e., $\partial r/\partial T_a = -a_1$ and $\partial r/\partial F$ is unchanged). In this case the

Table 2. The Slopes and Intercepts of the Lines Giving $\frac{dLE}{dT_a}$ and $\frac{dS}{dT_a}$ as a Function of $\frac{dF}{dT_a}$

Assumptions	Heat Flux	Slope	Intercept ($Wm^{-2}K^{-1}$)
Δr, $\Delta k = 0$ and $\Delta F = L\Delta E + \Delta S$	Latent	0.70	2.07
	Sensible	0.30	−2.07
$\Delta k = 0$ and $\Delta F = L\Delta E + \Delta S$	Latent	1.06	0.90
	Sensible	−0.06	−0.90
$\Delta F = L\Delta E + \Delta S$	Latent	1.06	0.75
	Sensible	−0.06	−0.75
None	Latent	1.06	0.39
	Sensible	−0.06	−0.90

change in latent heat flux is substantially greater than the case of constant relative humidity and, moreover *exceeds* the CC rate when the change in the net radiation is 2.9 W m^{-2} K^{-1} (Figure 5). Thus the CC rate increases in precipitation [*Wentz et al.*, 2007] do not necessarily imply that the changes in the net radiation at surface are approximately equal to the CC rate [*Allan and Soden*, 2007]. In Figure 5 we see that if the relative humidity decreases over the oceans, then the sensible heat flux and the net radiation play an equal role offsetting the CC rate increase in evaporation.

[31] Nevertheless it is important to note that the relative humidity increase appears to be a robust feature of global warming as 20 out of 22 models simulate increases in the mean near-surface relative humidity over the world's oceans (Figure 1). The remaining two models predict basically zero change in relative humidity. The largest increases in relative humidity outside the high latitudes are over the subtropical oceans (Figure 6a), which is consistent with *Richter and Xie* [2008]. On a regional basis, however, the relative humidity changes are not as robust as the global-mean case: less than 85% of the models agree that there is an increase in local relative humidity over most of the extratropical oceans, much of the tropical Atlantic, and portions of the tropical eastern Pacific (Figure 6a). In contrast to the relative humidity, the change in the local air-surface temperature difference (= $\Delta(T_s - T_a)$) is a significantly more robust feature over the world's oceans (Figure 6b). The change is −0.1°C to −0.2°C over most of the oceans equatorward of 45° latitude. For the oceans poleward of this latitude, the change tends to be larger in magnitude but the same sign.

[32] For further insight into the robustness of the increase in relative humidity with temperature, we look at perhaps the simplest model of the global hydrological cycle with predicted relative humidity [*Takahashi*, 2009]. This is an idealized radiative convective model that considers the energy budgets of the free atmosphere and the subcloud layer separately, which enables it to predict both the air-sea temperature difference and the surface relative humidity. The surface fluxes are parameterized by (1) and (2) with a constant k. We run the model for a range of optical depths with semigray radiation and a moist adiabatic lapse rate above the lifting condensation level. The surface relative humidity versus the temperature for this range of simulations is shown in Figure 7a. We see that for temperatures less than ~288 K the relative humidity decreases with temperature while for temperatures greater than ~288 K the relative humidity increases with temperature. The 288 K case is considered the control "earth-like" case by *Takahashi* [2009], so according to this model, earth is right at the transition between positive and negative $\frac{dr}{dT_a}$. While this model is too simple to draw specific quantitative predictions, it nevertheless suggests that it is possible for near-surface relative humidity to decrease under global warming. The effect of this relative humidity change and the air-sea temperature difference on $\frac{d\ln E}{dT_a}$ in (9) is shown in Figure 7b. The sum of these two terms gives the deviation of the E change from the CC rate. The magnitude of the relative humidity effect for $T_a \sim 285$ K is comparable to the models but opposite in sign. However, the difference between $\frac{dLE}{dT_a}$ and $\frac{dF}{dT_a}$ is less than 2 W m^{-2} K^{-1} in this model, while the differences in Figure 5 are over 3 Wm^{-2} K^{-1} for the case when E changes at the CC rate. The effect of $\frac{\partial r}{\partial F}$ on the slope of the $\frac{dLE}{dT_a}$ versus $\frac{dF}{dT_a}$ line is the main reason for this discrepancy.

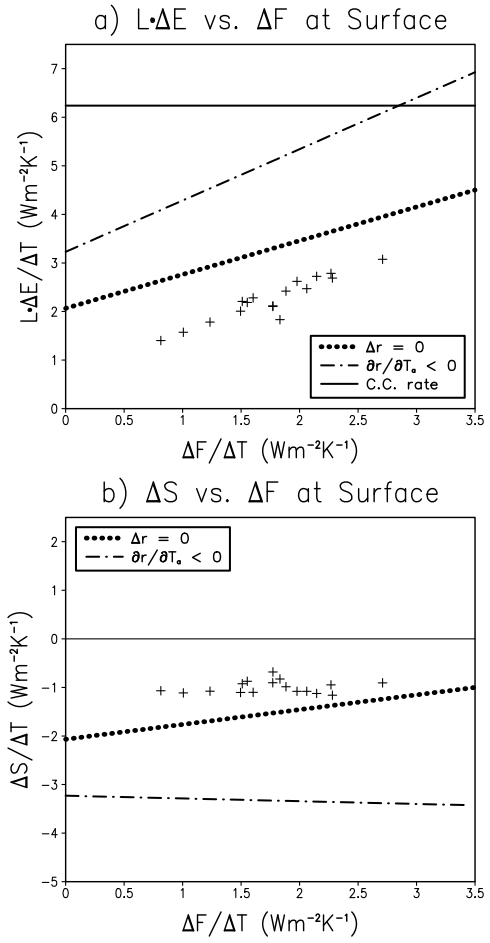

Figure 5. (a) Scatter plot of the change in latent heat flux per change in surface air temperature versus the change in net surface radiation per change in surface air temperature for 18 climate models (+ signs). The dotted line is the calculated relationship assuming relative humidity and k are constant and that the surface energy budget is balanced (15). The dashed line is the calculated relationship assuming that relative humidity decreases with temperature instead of increases ($\partial r/\partial T_a = -a_1$). The solid line is the CC rate. (b) The same as Figure 5a except for sensible heat instead of latent heat.

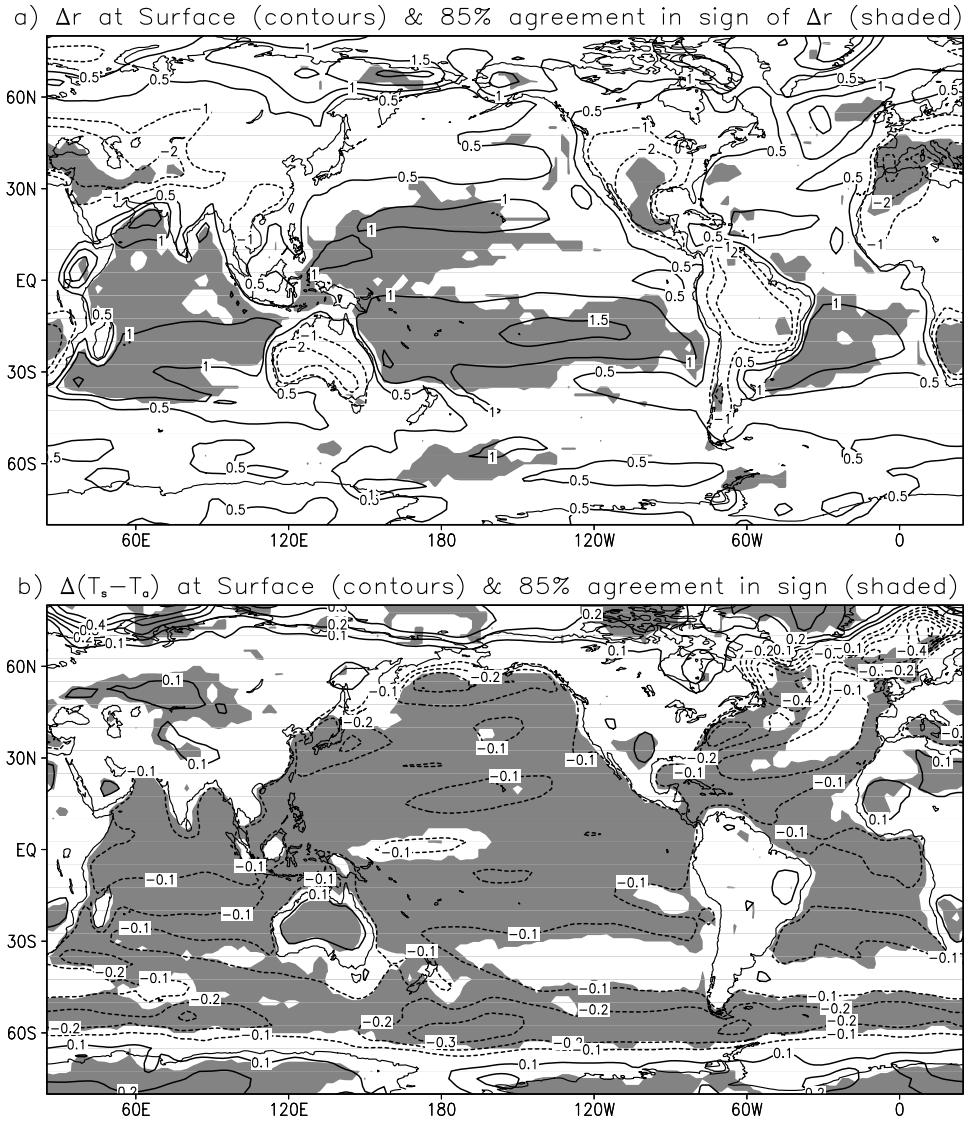

Figure 6. (a) The ensemble-mean change in annual-mean 1,000 mbar relative humidity for 22 climate models. The shading shows regions where over 85% of the models agree in the sign of the relative humidity change. (b) Same as Figure 6a but for the change in the air-surface temperature difference.

[33] *Takahashi*'s [2009] paper also provides a fundamentally different interpretation of the constraints on the hydrological cycle. Our framework considers the net surface radiation and the relative humidity (and k in the more complicated climate model case) as given and calculates the sensible and latent heat from this. In *Takahashi*'s [2009] model, one first calculates the radiative flux divergence in the free atmosphere and in the subcloud layer, and one then sets the latent heat flux to the radiative divergence in the free atmosphere (assumes no net condensation in the subcloud layer) and the sensible heat flux to the radiative divergence in the subcloud layer (assumes large-scale transport and entrainment of sensible heat above subcloud layer negligible). Therefore, the radiative fluxes determine everything, and the air-sea temperature difference and the near-surface specific humidity are simply that which produce the required sensible and latent heat fluxes, respectively. Like our framework, the air-sea temperature flux is diagnostic; the difference lies in the surface relative humidity, which is diagnostic in the paper by *Takahashi* [2009] but considered more fundamental in our case.

4.4. Results as Climate Approaches Equilibrium

[34] In the results above, we separated the contributions to latent and sensible heat change into the effect of relative humidity, k, and the net energy imbalance. If this is a useful decomposition then as equilibrium is attained, the net energy imbalance contribution should disappear while the relative humidity and k effects should remain relatively unchanged. We test this by repeating the analysis for the time periods 2180–2199 and 2280–2299 by which time the greenhouse gas concentrations have been fixed for about 100 and 200 years, respectively. Here we only show results for the nine models that are available out to 2300, so the values differ slightly from those in Table 2. Figure 8 shows the effect of relative humidity on the slope and intercept of

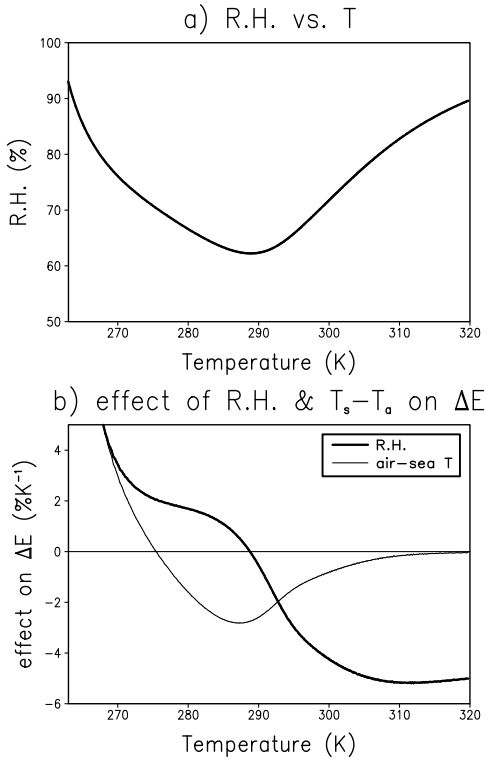

Figure 7. (a) The relative humidity as a function of surface air temperature for a range of simulations of the model of *Takahashi* [2009] with different optical depths. (b) The effect of relative humidity and the air-sea temperature difference on $\frac{d \ln E}{dT_a}$ as a function of temperature for the same range of simulations in Figure 7a.

the $\frac{dLE}{dT_a}$ versus $\frac{dF}{dT_a}$ line and the effect of k and net energy imbalance on the intercept of the $\frac{dLE}{dT_a}$ versus $\frac{dF}{dT_a}$line (k and net energy imbalance do not affect the slope). As equilibrium is reached, the effect of relative humidity on the slope increases by about 22% from 2100 to 2300, while the effect of relative humidity on the intercept to nearly constant over the time period. The k effect increases in magnitude by about 36% from 2100 to 2300. The change in the net energy imbalance effect, however, completely dominates the changes in the other terms as it decreases in magnitude by about a factor of 10. Similar results are obtained for the sensible heat flux. These results suggest that separating the latent and sensible heat change into the effect of relative humidity, k and the net energy imbalance is a useful decomposition.

5. Physical Mechanism of Relative Humidity/ Radiation Connection

[35] In the results above, the relative humidity change is given in terms the temperature and radiation change. Physically, the causality implied by the above linear fit is likely backwards (i.e., it is likely that the temperature and relative humidity change play a bigger role in setting the radiation change than vice versa). The temperature determines the radiation though changes in longwave emission, while the relative humidity determines the radiation through its effects on low-level cloudiness. Therefore, we fit the net radiation change to the change in temperature and relative humidity: $\Delta F = b_1 \Delta T_a + b_2 \Delta r$ (Figure 4b). Moreover, these ideas suggest that we should plot $\frac{\Delta E}{\Delta T_a}$ as a function $\frac{\Delta r}{\Delta T_a}$ instead of $\frac{\Delta F}{\Delta T_a}$ (Figure 9).

[36] Increased relative humidity leads to decreased E because of (1) the direct effect relative humidity on the air-sea specific humidity difference and (2) the indirect effect of relative humidity on cloudiness, and hence the net radiation at the surface. We calculate these two effects in Appendix D. Taking into account these two effects produces a good fit to the evaporation/relative humidity relationship in the climate models (solid line, Figure 9). If we assume that the radiation is independent of the relative humidity (i.e., $\frac{\partial F}{\partial r} \equiv b_2 = 0$), then we get the dashed line with slope −1.3 W m^{-2} %$^{-1}$ (Figure 9). Including the effect of relative humidity on radiation contributes an additional −1.0 Wm^{-2} %$^{-1}$ to the total slope (solid line). Hence, for a given relative humidity change, the effect of relative humidity on E via the net radiation is nearly the same magnitude as the effect of relative humidity on E via the air-sea specific humidity difference.

[37] In the results above, we fit the net radiation to the temperature and the low-level relative humidity. Because the low-level relative humidity is presumably affecting low-level clouds, one might expect the relative humidity to affect the shortwave more than the longwave contribution to the

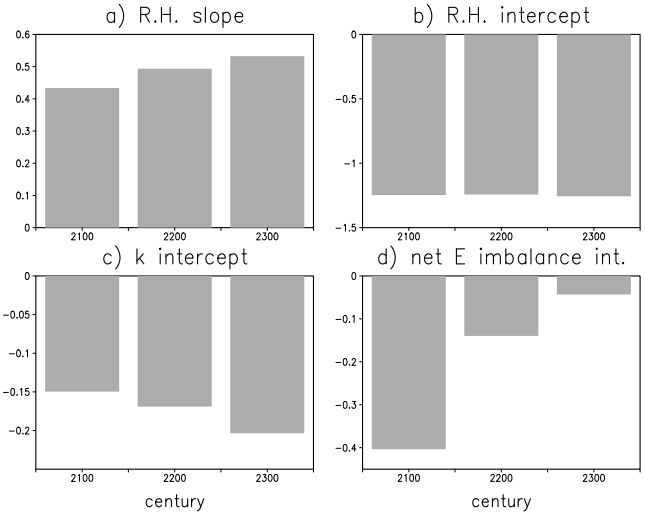

Figure 8. (a) The effect of relative humidity on the slope of the $\frac{dLE}{dT_a}$ versus $\frac{dF}{dT_a}$ line as a function of century. The vertical axis is measured in watts per meter squared per Kelvin. (b) The effect of relative humidity on the intercept of the $\frac{dLE}{dT_a}$ versus $\frac{dF}{dT_a}$ line. The vertical axis is measured in watts per meter squared. (c) The effect of k on the intercept of the $\frac{dLE}{dT_a}$ versus $\frac{dF}{dT_a}$ line. The vertical axis is measured in watts per meter squared. (d) The effect of a net energy imbalance on the intercept of the $\frac{dLE}{dT_a}$ versus $\frac{dF}{dT_a}$ line. The vertical axis is measured in watts per meter squared. Analysis is restricted to the nine models with data out to 2300: cccma_cgcm3_1, cccma_cgcm3_1_t63, cnrm_cm3, csiro_mk3_5, gfdl_cm2_0, gfdl_cm2_1, giss_model_e_r, miroc3_2_medres, and mri_cgcm2_3_2a.

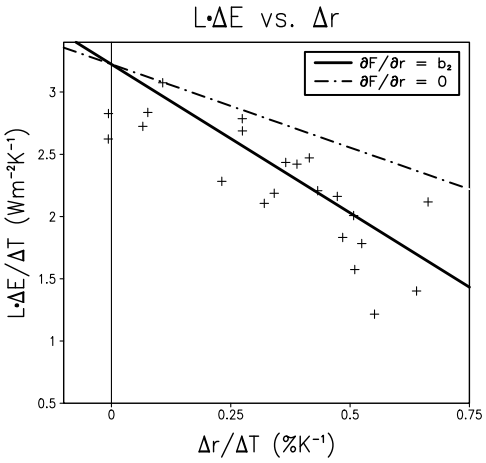

Figure 9. Scatter plot of the change in latent heat flux per change in surface air temperature versus the change in relative humidity per change in surface air temperature for 22 climate models (+ signs). The solid line is the calculated relationship assuming the net radiation depends on both temperature and relative humidity (and k is variable and the surface energy budget is not balanced) (D3). The dashed line is the calculated relationship assuming the net radiation only depends on temperature.

net radiation. Indeed, we find that the shortwave radiation is well correlated with the relative humidity while the longwave radiation is not (correlation is 0.47 for shortwave radiation versus 0.06 for longwave radiation). Furthermore, we find that the model-to-model variability in relative humidity change is correlated with the cloud-condensed-water-content change at the 0.70 level.

6. Discussion and Conclusions

[38] Changes in evaporation over the global oceans are investigated in climate models and through simple arguments involving the surface energy budget. It is shown that the dominant contributors to evaporation changes in global climate models include robust decreases in the air-sea temperature difference and increases in relative humidity. These two effects are the main contributors to the reduction in the evaporation increase below the CC rate. The change in evaporation in climate models is substantially smaller than the rate of increase expected if relative humidity and turbulent exchange coefficient, k, are constant. For example, for a fixed net radiation change of 1 W m^{-2} K^{-1}, the evaporation change in climate models is over a factor of two smaller than the case of fixed relative humidity and k (1.1% K^{-1} compared to 2.5% K^{-1}). This dramatic reduction in evaporation compared to the case with fixed relative humidity and k is associated with a change in the sensible heat flux. An increase in surface relative humidity is the largest contributor to this discrepancy, particularly for small increases in net radiation. An imbalance in the net energy at the surface is the second largest contributor to this discrepancy.

[39] A simple framework is presented in which the air-sea temperature difference adjusts to changes in relative humidity and atmospheric temperature, in order to maintain a consistent energy budget. In this framework the air-sea temperature difference is determined by changes in surface air temperature and relative humidity (or surface radiation), which are imposed in the present treatment. It is shown that the change in air-sea temperature difference leads to a nonnegligible change in sensible heat flux, which can be as large as changes in surface radiation, or latent heat flux [*Boer*, 1993; *Stephens and Ellis*, 2008; *O'Gorman and Schneider*, 2008].

[40] In addition, this paper clarifies the role of surface wind speed in the evaporation change observed in climate models. For example, *Wentz et al.* [2007] state that because evaporation in climate models increases less than the CC rate, the climate models must decrease global-mean wind speeds at the surface. This claim is overly simplistic because it neglects the importance of both the air-sea temperature difference and the relative humidity in reducing the evaporation change below the CC rate. Indeed, we have shown that 3 out of 14 climate models actually increase global-mean wind speeds over the oceans despite the fact that all climate models predict a substantial reduction in the evaporation change below the CC rate.

[41] Given the discrepancy between the "observed" precipitation trends and the climate model precipitation trends [*Wentz et al.*, 2007; *Allan and Soden*, 2007], one might hope that (9) would provide an alternative test of the observed changes in the hydrologic cycle. The variables in (9) that lead to an evaporation change different from the CC rate are the turbulent exchange coefficient, the air-sea temperature difference, and the relative humidity. Unfortunately, the changes in air-sea temperature difference and relative humidity in the climate models during the 20th century are very small and would therefore be impossible to distinguish, in observations, from the null hypothesis of no trend. For example, over the period from 1950 to 1999, the ensemble-mean climate model trends in $T_a - T_s$ and relative humidity are 0.0079 K/decade and 0.034%/decade, respectively. The trends in $T_a - T_s$ are about ten times smaller than the trends in T_a, and the trends in relative humidity are well below the statistical significance level also [*Willett et al.*, 2008].

[42] Because the relative humidity has an important effect on the evaporation change, the uncertainty in changes in the hydrologic cycle depend on uncertainties in relative humidity as well as uncertainties in net surface radiation. For example, if near-surface relative humidity decreases instead of increases with temperature, then the changes in evaporation would be substantially larger. While all of the current generation of climate models simulate either increases or no change in relative humidity, the simple model of *Takahashi* [2009] suggests that decreasing relative humidity under global warming is not impossible. The above discussion suggests that an accurate representation of boundary-layer humidity is very important for simulating changes in the hydrologic cycle.

Appendix A: Mechanisms of Evaporation Change

[43] In this appendix, we derive the contributions of the air-sea temperature difference, the relative humidity, and k to the fractional change in evaporation over the oceans using the bulk formula for evaporation (1). First, we take the

logarithm and the derivative with respect to air temperature of (1):

$$\frac{d\ln E}{dT_a} = \frac{\left.\frac{dq_s}{dT}\right|_{T=T_s}\frac{dT_s}{dT_a} - r\left.\frac{dq_s}{dT}\right|_{T=T_a} - \frac{dr}{dT_a}q_s(T_a)}{q_s(T_s) - rq_s(T_a)} + \frac{d\ln k}{dT_a}. \quad \text{(A1)}$$

The CC rate, α, is defined as the fractional change in q_s per degree temperature change: $\alpha = \frac{1}{q_s}\frac{dq_s}{dT}$ (we assume that the pressure is constant so that $\frac{dq_s}{dT} = \frac{\partial q_s}{\partial T}$). Substituting this into (A1) and defining γ to be $\frac{dT_s}{dT_a}$, we have

$$\frac{d\ln E}{dT_a} = \frac{\alpha q_s(T_s)\gamma - r\alpha q_s(T_a) - \frac{dr}{dT_a}q_s(T_a)}{q_s(T_s) - rq_s(T_a)} + \frac{d\ln k}{dT_a}. \quad \text{(A2)}$$

We assume that α is constant in (A2) so that $\alpha(T_s) = \alpha(T_a)$. Adding and subtracting $\alpha q_s(T_s)$ to the numerator of the first term on the right and simplifying, we get

$$\frac{d\ln E}{dT_a} = \alpha - \frac{(1-\gamma)\alpha q_s(T_s)}{q_s(T_s) - rq_s(T_a)} - \frac{\frac{dr}{dT_a}q_s(T_a)}{q_s(T_s) - rq_s(T_a)} + \frac{d\ln k}{dT_a}. \quad \text{(A3)}$$

Appendix B: Sensitivity of Net Radiation to Air-Sea Temperature Difference

[44] In the discussion in Appendix A, the net radiation is considered given, and we allow the air-sea temperature difference to vary in order to bring the latent and sensible heat change into equilibrium with the net radiation change. If the net radiation depends strongly on the air-sea temperature difference, then we are not justified in assuming the net radiation is fixed while the latent and sensible heat adjust to bring the energy budget into equilibrium. Here, we test the validity of this assumption.

[45] To gauge the sensitivity of the net radiation, the latent heat and the sensible heat to the air-sea temperature difference, we take the derivative of each of these quantities with respect to the surface temperature while holding the air temperature fixed. For simplicity, we assume relative humidity and k are constant below. Using (1) and (2) for the latent and sensible heat, we have

$$L\left.\frac{dE}{dT_s}\right|_{T_a=const} = kL\alpha q_s(T_s), \quad \text{(B1)}$$

$$\left.\frac{dS}{dT_s}\right|_{T_a=const} = kc_p. \quad \text{(B2)}$$

We assume that the net radiation change is dominated by the longwave radiation, and we use the Stefan-Boltzmann law for the upwelling and downwelling longwave radiation. Because only the upwelling radiation depends directly on the surface temperature, we have

$$\left.\frac{dF}{dT_s}\right|_{T_a=const} = 4\sigma T_s^3. \quad \text{(B3)}$$

Substituting numbers in (B1), (B2), and (B3), we find that the sum of the latent and sensible heat change is 42.1 W m^{-2} K^{-1}, while the net radiation change is 5.7 W m^{-2} K^{-1}. Hence assuming that the change in radiation with air-sea temperature difference is small compared to the latent and sensible heat is a reasonable first-order approximation. If the shortwave change opposes the longwave change as in the global warming runs, then (B3) overestimates the sensitivity of radiation to air-sea temperature difference, and the validity of the above approximation is even greater.

Appendix C: Effect of Turbulent Exchange Coefficient and Imbalanced Energy Budget on the Latent and Sensible Change

[46] In this appendix we calculate the effect of changes in k and imbalances in the surface energy budget on the changes in the latent and sensible heat fluxes. To calculate the effect of k on the latent and sensible heat, we follow the same procedure as for the relative humidity except that we first take the logarithm of k and we only use the temperature as a predictor: $\Delta \ln k = a_3\Delta T_a$. The coefficient a_3 is determined via linear regression ($a_3 = -6.9 \times 10^{-3}$ K^{-1}), and defines the value of $\frac{d\ln k}{dT_a}$.

[47] Since the energy budget is not balanced under a transient increase in greenhouse gases, we write (11) as

$$F = kc_p(T_s - T_a) + kL(q_s(T_s) - rq_s(T_a)) + \varepsilon, \quad \text{(C1)}$$

where ε is the residual. We fit $\Delta\varepsilon$ to ΔT_a ($\Delta\varepsilon = a_4\Delta T_a$) and define $\frac{d\varepsilon}{dT_a}$ as a_4 ($a_4 = 0.51$ W m^{-2} K^{-1}). We then take the derivative of (C1) with respect to T_a, and substitute a_1 for $\frac{\partial r}{\partial T_a}$, a_2 for $\frac{\partial r}{\partial F}$, a_3 for $\frac{d\ln k}{dT_a}$, and a_4 for $\frac{d\varepsilon}{dT_a}$. After some algebra, γ and the sensible and latent heat changes with variable relative humidity and k, and imbalanced energy budget are

$$\gamma = \tilde{\gamma} - \frac{(S+LE)\frac{d\ln k}{dT_a} + \frac{d\varepsilon}{dT_a}}{kc_p + kL\alpha q_s(T_s)}, \quad \text{(C2)}$$

$$\frac{dS}{dT_a} = \frac{d\tilde{S}}{dT_a} + \frac{\left(L\alpha q_s(T_s)S - c_pLE\right)}{c_p + L\alpha q_s(T_s)}\frac{d\ln k}{dT_a} - \frac{c_p}{c_p + L\alpha q_s(T_s)}\frac{d\varepsilon}{dT_a}, \quad \text{(C3)}$$

$$L\frac{dE}{dT_a} = L\frac{d\tilde{E}}{dT_a} - \frac{\left(L\alpha q_s(T_s)S - c_pLE\right)}{c_p + L\alpha q_s(T_s)}\frac{d\ln k}{dT_a} - \frac{L\alpha q_s(T_s)}{c_p + L\alpha q_s(T_s)}\frac{d\varepsilon}{dT_a}, \quad \text{(C4)}$$

where the tilde refers to the corresponding quantities in (16), (17), and (18), which assume that k is constant and the energy budget is balanced.

Appendix D: Change in Latent and Sensible Heat in Terms of the Change in Relative Humidity

[48] In this appendix we calculate the change in latent and sensible heat in terms of the change in relative humidity. First, we take the derivative of (C1) with respect to T_a,

replacing $\frac{dF}{dT_a}$ with $\frac{\partial F}{\partial r}\frac{dr}{dT_a}+\frac{\partial F}{\partial T_a}$. We also allow k to vary and the energy budget to be imbalanced as before. After some algebra, we get

$$\gamma=\frac{\frac{\partial F}{\partial T_a}+\frac{\partial F}{\partial r}\frac{dr}{dT_a}+kc_p+kL\alpha rq_s(T_a)+kLq_s(T_a)\frac{dr}{dT_a}-(S+LE)\frac{d\ln k}{dT_a}-\frac{d\varepsilon}{dT_a}}{kc_p+kL\alpha q_s(T_s)}, \tag{D1}$$

$$\frac{dS}{dT_a}=\frac{c_p}{c_p+L\alpha q_s(T_s)}\cdot\left[\frac{\partial F}{\partial T_a}+\frac{\partial F}{\partial r}\frac{dr}{dT_a}-kL\alpha(q_s(T_s)-rq_s(T_a))+kLq_s(T_a)\frac{dr}{dT_a}-LE\frac{d\ln k}{dT_a}-\frac{d\varepsilon}{dT_a}\right]+\frac{L\alpha q_s(T_s)}{c_p+L\alpha q_s(T_s)}S\frac{d\ln k}{dT_a}, \tag{D2}$$

$$L\frac{dE}{dT_a}=\frac{c_p}{c_p+L\alpha q_s(T_s)}\cdot\left[kL\alpha(q_s(T_s)-rq_s(T_a))-kLq_s(T_a)\frac{dr}{dT_a}+LE\frac{d\ln k}{dT_a}\right]+\frac{L\alpha q_s(T_s)}{c_p+L\alpha q_s(T_s)}\left[\frac{\partial F}{\partial T_a}+\frac{\partial F}{\partial r}\frac{dr}{dT_a}-S\frac{d\ln k}{dT_a}-\frac{d\varepsilon}{dT_a}\right]. \tag{D3}$$

As above, the coefficients in the linear fit, $\Delta F = b_1\Delta T_a + b_2\Delta r$, define the values for $\frac{\partial F}{\partial T_a}$ and $\frac{\partial F}{\partial r}$. Equations (D2) and (D3)) give the change in sensible and latent heat in terms of the change in relative humidity (i.e., the net radiation is not an independent variable but is determined by the temperature and relative humidity).

[49] **Acknowledgments.** We acknowledge the international modeling groups for providing their data for analysis, the Program for Climate Model Diagnosis and Intercomparison (PCMDI) for collecting and archiving the model data, the JSC/CLIVAR Working Group on Coupled Modeling (WGCM) and their Coupled Model Intercomparison Project (CMIP) and Climate Simulation Panel for organizing the model data analysis activity, and the IPCC WG1 TSU for technical support. The IPCC Data Archive at Lawrence Livermore National Laboratory is supported by the Office of Science, U.S. Department of Energy. Support for this research comes from the National Science Foundation (NSF) as a Drought in Coupled Models Project (DRICOMP) grant (NSF ATM 0739846) under the U.S. CLIVAR Program (Lorenz), and the Office of Science (BER), U. S. Department of Energy, grant DE-FG02-07ER64434 (DeWeaver). DeWeaver's work was also supported by the NSF during his employment there.

References

Allan, R. P., and B. J. Soden (2007), Large discrepancy between observed and simulated precipitation trends in the ascending and descending branches of the tropical circulation, *Geophys. Res. Lett.*, *34*, L18705, doi:10.1029/2007GL031460.

Allen, M. R., and W. J. Ingram (2002), Constraints on future changes in climate and the hydrological cycle, *Nature*, *419*, 224–232.

Boer, G. J. (1993), Climate change and the regulation of the surface moisture and energy budgets, *Clim. Dyn.*, *8*, 225–239.

Bolton, D. (1980), The computation of equivalent potential temperature, *Mon. Weather Rev.*, *108*, 1046–1053.

Held, I. M., and B. J. Soden (2006), Robust responses of the hydrological cycle to global warming, *J. Clim.*, *19*, 5686–5699.

IPCC (2001), *Climate Change 2001: The Scientific Basis*, contribution of Working Group I to the Third Assessment Report of the Intergovernmental Panel on Climate Change, edited by J. T. Houghton et al., 881 pp., Cambridge University Press, Cambridge.

Lambert, F. H., A. R. Stine, N. Y. Krakauer, and J. C. H. Chiang (2008), How much will precipitation increase with global warming? *EOS*, *89*, 193–194.

Lambert, F. H., and M. R. Allen (2009), Are changes in global precipitation constrained by the tropospheric energy budget? *J. Clim.*, *22*, 499–517.

Lu, J. H., and M. Cai (2009), Stabilization of the atmospheric boundary layer and the muted global hydrological cycle response to global warming, *J. Hydrometeorol.*, *10*, 347–352.

O'Gorman, P. A., and T. Schneider (2008), The hydrological cycle over a wide range of climates simulated with an idealized GCM, *J. Clim.*, *21*, 3815–3832.

Pierrehumbert, R. T. (2002), The hydrological cycle in deep-time climate problems, *Nature*, *419*, 191–198.

Previdi, M., and B. G. Liepert (2008), Interdecadal variability of rainfall on a warming planet, *EOS*, *89*, 193, 195.

Richter, I., and S.-P. Xie (2008), Muted precipitation increase in global warming simulations: A surface evaporation perspective, *J. Geophys. Res.*, *113*, D24118, doi:10.1029/2008JD010561.

Stull, R. B. (1989), *An introduction to boundary layer meteorology*, 2nd ed., 685 pp., Springer.

Stephens, G. L., and T. D. Ellis (2008), Controls of global-mean precipitation increases in global warming GCM experiments, *J. Clim.*, *21*, 6141–6155.

Takahashi, K. (2009), Radiative constraints on the hydrological cycle in an idealized radiative-convective equilibrium model, *J. Atmos. Sci.*, *66*, 77–91.

Wentz, F. J., L. Ricciardulli, K. Hilburn, and C. Mears (2007), How much more rain will global warming bring? *Science*, *317*, 233–235.

Willett, K. M., P. D. Jones, N. P. Gillett, and P. W. Thorne (2008), Recent changes in surface humidity: Development of the HadCRUH dataset, *J. Clim.*, *21*, 5364–5383.

E. T. DeWeaver, D. J. Lorenz, and D. J. Vimont, Center for Climatic Research, 1225 W. Dayton St., Madison, WI 53706, USA. (dlorenz@wisc.edu)